Aromatic Pathways of Porphins, Chlorins, and Bacteriochlorins

Heike Fliegl*[,†,‡] and Dage Sundholm*[,‡]

†Centre for Theoretical and Computational Chemistry (CTCC), Department of Chemistry, University of Oslo, P.O. Box 1033 Blindern, 0315 Oslo, Norway

‡Department of Chemistry, University of Helsinki, P.O. Box 55 (A.I. Virtanens plats 1), FIN-00014, University of Helsinki, Finland

Ⓢ *Supporting Information*

ABSTRACT: Magnetically induced current densities have been calculated for free-base porphynoids using the gauge including magnetically induce current (GIMIC) method. Numerical integration of the current density passing selected chemical bonds yields current pathways and the degree of aromaticity according to the magnetic criterion. The ring-current strengths of the porphins, chlorins, and bacteriochlorins are 1.5–2.5 times stronger than for benzene. The calculations show that the 18π [16]annulene inner cross is not the correct picture of the aromatic pathway for porphyrins. All conjugated chemical bonds participate in the current transport independently of the formal number of π electrons. The ring current branches at the pyrrolic rings taking both the outer and the inner route. The NH unit of the pyrrolic rings has a larger resistance and a weaker current strength than the pyrroles without inner hydrogens. The traditional 18π [18]annulene with inactive NH bridges is not how the ring-current flows around the macroring. The porphins have the strongest ring current of ca. 27 nA/T among the investigated porphynoids. The current strengths of the chlorins and bacteriochlorins are 19–24 nA/T depending on whether the ring current is forced to pass an NH unit or not. The current strengths of the 3-fold and 4-fold β-saturated porphynoids are 13–17 nA/T, showing that the inner-cross 18π [16]annulene pathway is not a preferred current route.
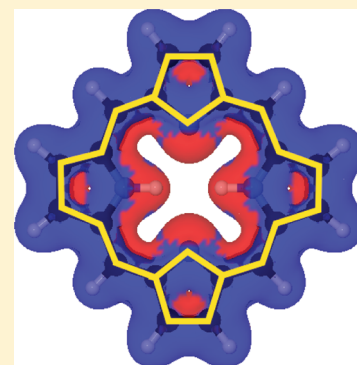
1. INTRODUCTION

An external magnetic field applied perpendicularly to a planar aromatic molecular ring induces a net diatropic current that flows around the ring. In aromatic molecules consisting of fused conjugated rings, the current can circle around one or several of the individual rings. It can also flow around the entire molecule. Thus, molecules with fused aromatic rings have many feasible current pathways, the routes of which are difficult to determine. It is not possible to determine magnetically induced current pathways experimentally. The only reliable means to elucidate the pathways of the current flow is to explicitly calculate the strength of the currents passing selected chemical bonds of the multiring molecule.

Porphyrins, which are aromatic molecules with 26 π electrons, consist of four pyrrole units connected by conjugated C–C bonds to form a larger ring with several possible aromatic pathways. Traditionally, porphyrins have been considered as a bridged 18π [18]annulene with the inner NH groups acting as inert bridges.[1–5] Cyrañski et al.[6] studied the aromatic pathway of free-base porphyrin (porphin) using nucleus independent chemical shifts[7] (NICS) and calculations of harmonic oscillator model of aromaticity[8] (HOMA) indices. They concluded that the aromatic pathway of porphins consists of the 18π [16]annulene internal cross implying that the ring current does not pass the outer C$_2$H$_2$ groups of the pyrrolic rings. Using current–density plots, Havenith et al. found more recently that the ring current avoids the outer route at the pyrroles without an inner hydrogen.[9] Other possible pathways for the induced ring current in porphyrins also exist. However,

they have to fulfill the Hückel rule for aromaticity involving $(4n+2)$ π electrons.[10,11] For porphyrins, Hückel-aromatic pathways might involve 18 π or 22 π electrons. Jusélius and Sundholm found that all 26 π electrons play an active role for the aromaticity of porphyrins.[12]

Chlorins and bacteriochlorins have 24 π and 22 π electrons as they are free-base porphynoids with one and two of the pyrrole rings saturated in the β positions, respectively. Jusélius and Sundholm calculated long-range magnetic shielding functions and used their aromatic ring current shieldings (ARCS) approach to estimate current strengths and current pathways in such free-base porphynoids.[13] In the ARCS studies, they found that the total aromatic pathways of the porphynoids and of magnesium porphyrin must be considered as a superposition of several pathways.[12,14] Thus, the aromaticity of the classical porphynoids is not yet settled, not to speak of more general porphyrinoids. Modern porphyrinoid chemistry also involves complicated molecules with singly and doubly twisted Möbius structures,[15–22] whose degree of aromaticity is very difficult to assess.[20,23–37]

The aim of this work is to employ the gauge-including magnetically induced current (GIMIC) method to elucidate the aromatic pathways of planar porphins, chlorins, and bacteriochlorins.[38–40] Compared to the previously employed NICS and ARCS methods, the GIMIC approach is more accurate. Thus, it avoids speculation about the current density, current strengths,

and aromatic pathways. The GIMIC method provides accurate quantitative information about the magnetically induced current density in molecular systems. Presently, such information is not possible to deduce from experimental data. Magnetically induced current densities of porphynoids have previously been calculated using the less accurate CTOCD-DZ method.[41,42] The current densities were plotted in planes parallel to porphynoids without any attempts to determine the explicit strength of the currents along various pathways.[5,43,44] Here, the current strengths and current pathways for different tautomers of the porphynoids are obtained by performing numerical integration of the current densities passing selected chemical bonds. The calculated current strengths and pathways are compared to the current strengths estimated from magnetic shieldings using the ARCS method.[12] Different aspects concerning the aromaticity of porphynoids are studied through systematically modifying the macroring by saturating one or several pyrrolic units at the β carbon positions. The $\pi-\pi$ conjugation of the $C_\beta-C_{\beta'}$ bond in the pyrrolic rings can efficiently be prevented through saturation of the β carbons. In that way, the current can be forced to take predetermined routes as one can expect that the current flow along the $C_\beta-C_{\beta'}$ bond is reduced upon saturation. The influence of the saturation on the current strengths can also be assessed.

This article is structured as follows. The computational methods are described in section 2. The molecular structures and the employed nomenclature are given in section 3.1. The aromatic pathways and the ring current strengths of the porphynoids are discussed in section 3.2. Finally, the main results and conclusions are given in section 4.

2. COMPUTATIONAL METHODS

The molecular structures of the studied molecules have been taken from previous work.[12] They were optimized at the density functional theory (DFT) level using the Becke−Perdew (BP) functional[45−47] and the resolution-of-the-identity approximation.[48] The Karlsruhe split-valence (def2-SVP) basis sets augmented with polarization functions on C and N were employed.[49,50] Nuclear magnetic shieldings have been calculated using Becke's three-parameter functional combined with the Lee−Yang−Parr exchange-correlation functional (B3LYP)[51,52] and the Karlsruhe triple-ζ quality basis set augmented with polarization functions (def2-TZVP).[53] The calculations have been performed using TURBOMOLE version 6.3.[54] The prefix def2 is omitted in further discussion.

Magnetically induced current densities were calculated using the GIMIC method.[38,39] GIMIC is an independent program that uses basis set information as well as the perturbed and unperturbed density matrices from nuclear magnetic shielding calculations as input data.[38] Since gauge-including atomic orbitals (GIAO) are employed,[55−58] accurate gauge-independent current densities are obtained with SVP quality basis sets. Here, the ring-current susceptibilities (in nA/T) are calculated using the Karlsruhe TZVP basis set.[53] The ring-current susceptibility, denoted in the following as ring-current strengths, can be used as a reliable measure of the molecular aromaticity. The current strengths are obtained by numerical integration of the current density passing through cut planes perpendicularly to selected bonds of the molecular system. The ring-current strength for benzene calculated at the B3LYP/TZVP level is 11.8 nA/T, which can be used as reference value for a typical aromatic molecule. Calculations of the current strength for selected bonds yield the electron-delocalization pathways responsible for the current transport around the macromolecular ring. Thus, GIMIC calculations provide detailed information about molecular aromaticity and current pathways.[37,59−61] The sign and magnitude of the obtained ring currents indicate whether molecular rings are aromatic, antiaromatic, or nonaromatic, thus having diatropic, paratropic, or vanishing net ring current.[62] Diatropic ring currents are

defined to generate a magnetic field opposing the applied field, whereas paratropic currents circulate in the opposite (nonclassical) direction strengthening the external magnetic field.[38,63−65] The GIMIC method including demonstrations of its applicability has recently been reviewed in a perspective article.[40] Current density plots were made with Jmol,[66] and the current strength profiles were obtained using gnuplot[67] and gimp.[68]

3. RESULTS AND DISCUSSION

3.1. Molecular Structures. The molecular structures of the porphynoids have been chosen such that the ring current is systematically constrained to flow along certain pathways. Desired current pathways can be achieved by saturating one or several pyrrolic units at the β positions, which interrupts the $\pi-\pi$ conjugation at the $C_\beta-C_{\beta'}$ bond. The magnetically induced current densities have been investigated for the following porphins and chlorins: *trans*-porphin (t-PH$_2$), *cis*-porphin (c-PH$_2$), *trans*-chlorin (t-CH$_2$-a and t-CH$_2$-b), *cis*-chlorin (c-CH$_2$-a and c-CH$_2$-b), where *cis* and *trans* refer to the positions of the inner hydrogens. The chlorins denoted t-CH$_2$-a and c-CH$_2$-a do not have any inner hydrogens connected to the pyrrolic ring that is saturated in the β positions, whereas t-CH$_2$-b and c-CH$_2$-b have one inner hydrogen connected to the β-saturated ring. The molecular structures of the porphins and the chlorins are shown in Figures 1 and 2, respectively.
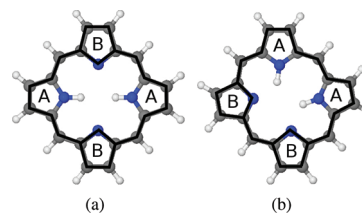

Figure 1. Molecular structures of the porphins. The dominating current pathways for (a) *trans*-porphin (t-PH$_2$) and (b) *cis*-porphin (c-PH$_2$) as obtained in the GIMIC calculations are indicated in black.
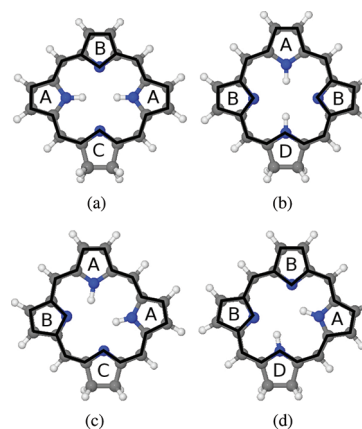

Figure 2. The molecular structures of the chlorins. The dominating current pathways for *trans*-chlorin (a) t-CH$_2$-a, (b) t-CH$_2$-b and *cis*-chlorin, (c) c-CH$_2$-a, and (d) c-CH$_2$-b as obtained in the GIMIC calculations are indicated in black.

Three bacteriochlorins and one isobacteriochlorin have been studied. The bacteriochlorins have two opposite pyrrolic rings saturated in the β positions, whereas for isobacteriochlorin two adjacent pyrrolic rings are saturated in the β positions. Two of the bacteriochlorins have inner hydrogens in *trans* position. For *trans*-bacteriochlorins (t-BCH$_2$-a), the inner hydrogens are

connected to the unsaturated pyrrolic rings. The other *trans*-bacteriochlorin (t-BCH$_2$-b) has the inner hydrogens connected to the β-saturated rings. For *cis*-bacteriochlorin (c-BCH$_2$), the inner hydrogens are in the *cis* position. For isobacteriochlorin only one tautomer is considered, namely, the one with the inner hydrogens in *trans* position (t-IBCH$_2$). Thus, t-IBCH$_2$ and c-BCH$_2$ have one of the inner hydrogens connected to a β-saturated ring. The molecular structures of the bacteriochlorins are shown in Figure 3.
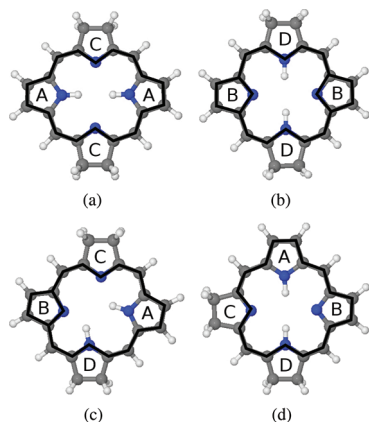

Figure 3. Molecular structures of the studied bacteriochlorins. The dominating current pathways for *trans*-bacteriochlorin (a) t-BCH$_2$-a, (b) t-BCH$_2$-b, for (c) *cis*-bacteriochlorin (c-BCH$_2$), and for (d) *trans*-isobacteriochlorin (t-IBCH$_2$) as obtained in the GIMIC calculations are indicated in black.

The porphynoids denoted t-3BCH$_2$ consist of three β-saturated pyrrolic rings with the inner hydrogens in the *trans* position. For t-3BCH$_2$-a, one of the inner hydrogens is connected to the unsaturated ring, whereas for t-3BCH$_2$-b both hydrogens are connected to the β-saturated rings. The molecule denoted t-4BCH$_2$ has all four pyrrolic rings saturated in the β positions with the inner hydrogen in the *trans* position. The structures of t-3BCH$_2$-a, t-3BCH$_2$-b, and t-4BCH$_2$ are shown in Figure 4.
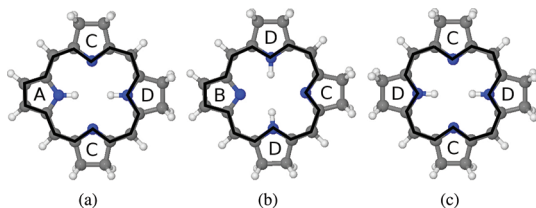

Figure 4. Molecular structures of the porphynoids with 3-fold and 4-fold β-saturated pyrrole rings. The dominating current pathways for *trans*-porphynoids (a) t-3BCH$_2$-a, (b) t-3BCH$_2$-b, and (c) t-4BCH$_2$ as obtained in the GIMIC calculations are indicated in black.

3.2.1. Aromatic Pathways. *Porphins.*

The ring-current strengths and the aromatic pathways were obtained by calculating the current strength passing specific chemical bonds. The net ring-current strengths for the porphins of 27.5 nA/T (t-PH$_2$) and 27.1 nA/T (c-PH$_2$) are more than twice the benzene value. The integrated current strength is significantly larger than the one of 10.4 nA/T deduced from the long-range magnetic shieldings using the ARCS approach.[12] The diatropic contribution of about 30 nA/T is almost an order

of magnitude larger than the paratropic one. The employed molecular structure has little influence on the ring-current strengths. Current density calculations using a molecular structure optimized at the B3LYP/TZVP level yield current strengths that deviate by less 0.2 nA/T from the values obtained using the BP/SVP structure.

The calculations show that the ring current splits into an outer and inner pathway at each pyrrolic ring. The calculated currents show that the inner hydrogens have high resistance, because the strength of the ring current passing the NH moiety of 7.8−8.5 nA/T is about half the one of nearly 19 nA/T that takes the outer route via the β carbons. For the pyrrolic rings without an inner hydrogen, the ring current is more evenly divided between the two routes. The strength of the current along the inner pathway is 15 nA/T, which is 3 nA/T larger than for the outer route.

The current density plots in Figure 5 show that the diatropic current density flows along the outer edge of the molecule,
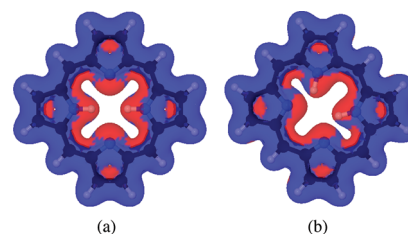

Figure 5. Magnetically induced current density calculated for (a) *trans*-porphin (t-PH$_2$) and (b) *cis*-porphin (c-PH$_2$). Diatropic currents are shown in blue and paratropic currents in red.

whereas a continuous paratropic current passes along the interior part of the macroring. The current strength profile for t-PH$_2$ is depicted in Figure 6. It confirms that a very weak paratropic current circles inside the pyrrolic rings. The paratropic current inside the pyrrolic ring with an inner hydrogen is somewhat stronger than for the one without it. However, the paratropic currents of −1.4 nA/T in the pyrrolic rings are very weak as compared to the ring current of about 27 nA/T flowing around the porphin. The strength of the ring current around the pyrrolic rings, estimated from the current passing perpendicularly to the C$_\alpha$−C$_{meso}$ bonds on both sides of the pyrrolic ring, is very weak. The weak ring currents of the pyrrole rings cannot explain the increase in the magnetic shielding above the pyrrolic rings obtained in the magnetic shielding calculations.[12] The dominating ring current pathways for t-PH$_2$ and c-PH$_2$ are shown in Figure 1. The current strengths of the different pathways are given in Table 1.

Porphin is a good example showing the importance of performing numerical integration of the strength of the ring current passing selected bonds. The integration yields explicit values for the current strength, which unambiguously show how the currents flow in the molecular ring. Assessing the aromaticity by using current plots and the maximum current strength calculated in the plotting plane might lead to incorrect conclusions. Havenith et al.[9] plotted the current density obtained using the CTOCD-DZ method.[41,42] They found that the total ring current of porphin is twice the benzene value. It is bifurcated in the two pyrroles with inner hydrogens and that it avoids the outer C$_2$H$_2$ moieties of the other two pyrroles. The integration of the current strengths yields a completely different picture with bifurcations at all pyrroles and strong
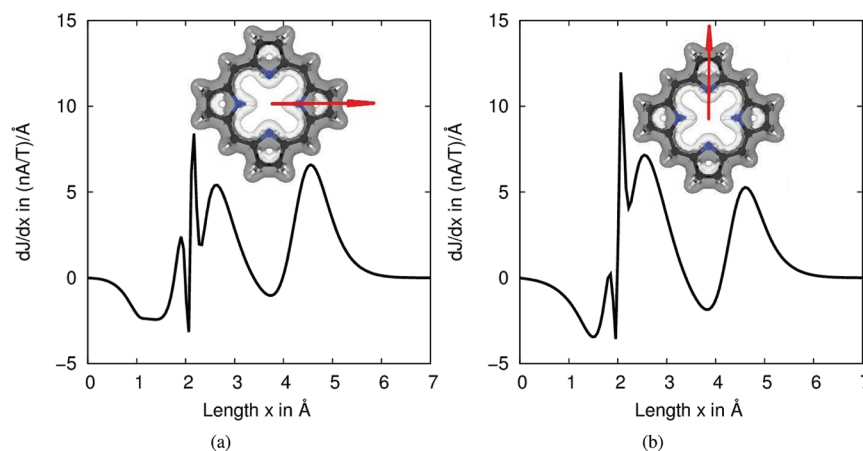
Figure 6. Ring−current profiles for t-PH$_2$ calculated from the center of the molecule through the center of one of the pyrrolic rings.

Table 1. Strength of the Magnetically Induced Currents (in nA/T) Flowing around the Macroring as well as along the C=C (or C−C) and C−N−C Routes of the Pyrrolic Rings of *trans*-Porphin (t-PH$_2$) and *cis*-Porphin (c-PH$_2$)^a

			route	
molecule	ring	macroring	C−N−C	C=C
t-PH$_2$	A^H	27.2	7.8	19.4
	B	27.5	15.2	12.3
c-PH$_2$	A^H	27.0	8.5	18.5
	B	27.1	15.0	12.1

^{a}Pyrrolic rings with inner hydrogens are denoted by a superscript *H*. See Figure 1.

Table 2. Strength of the Magnetically Induced Currents (in nA/T) Flowing around the Macroring as well as along the C=C (or C−C) and C−N−C Routes of the Pyrrolic Rings of *trans*-Chlorin (t-CH$_2$-a, t-CH$_2$-b) and *cis*-Chlorin (c-CH$_2$-a, c-CH$_2$-b)^a

			route	
molecule	ring	macroring	C−N−C	C=C
t-CH$_2$-a	A^H	24.0	6.3	17.7
	B	23.9	11.2	12.7
	C	24.1	23.2	0.9
t-CH$_2$-b	A^H	19.2	3.3	15.9
	B	19.5	8.5	11.0
	D^H	19.5	19.9	−0.4
c-CH$_2$-a	A^H	19.4	1.4	18.0
	B	19.7	9.7	10.0
	C	19.9	18.5	1.4
c-CH$_2$-b	A^H	19.5	3.6	15.9
	B	19.5	8.2	11.3
	D^H	19.7	19.9	−0.2

^{a} The A−D labeling of the pyrrolic rings is given in Figure 2. Pyrrolic rings with inner hydrogens are denoted by a superscript *H*.

currents along all possible pathways. The current of 12.3 nA/T flowing via the C$_2$H$_2$ route of the pyrroles without an inner hydrogen is actually stronger than the ring current of benzene.

3.2.2. Chlorins. Chlorins have one pyrrolic ring saturated in the β positions, which is expected to prevent the ring current from taking that route. The current strength and current pathways were calculated for the four chlorin tautomers with the inner hydrogens in different positions. The dominating ring-current pathways are shown in Figure 2, which shows that the ring-current pathway is split into outer and inner routes at the pyrrolic rings. The strongest net ring current of ca. 24 nA/T is obtained for *trans*-chlorin t-CH$_2$-a, where the ring current is not forced to pass any inner NH moiety, whereas for t-CH$_2$-b the high resistance of the NH unit reduces the current strength to about 19.5 nA/T, when the passage via the β positions of the pyrrolic ring with an inner hydrogen is practically blocked by saturated β carbons. The current strengths of the different pathways are given in Table 2.

For t-CH$_2$-a, the strongest current of 17.7 nA/T passes the outer route at ring A, which has an inner hydrogen, whereas the current of 6.3 nA/T via the NH unit is much weaker. The ring current is almost equally distributed along the two paths at ring B, which has no inner hydrogen. The outer route has a current strength of 12.7 and 11.2 nA/T for the inner one. For ring C, almost the entire current of 23.2 nA/T passes the nitrogen, whereas only 0.9 nA/T crosses the saturated C$_\beta$−C$_{\beta'}$ bond. For c-CH$_2$-a, the current strengths and pathways are very similar to those obtained for t-CH$_2$-a. The current passing ring B is equally split into 9.7 nA/T via the inner route and 10.0 nA/T taking the outer route. t-CH$_2$-b, c-CH$_2$-a, and c-CH$_2$-b have similar net ring-current strengths. The ring currents are though

weaker than for t-CH$_2$-a. The inner hydrogen at ring A directs the main current flow of 15.9−18.0 nA/T to the outer route. The ring current splits at ring B into an outer and inner pathway with almost equal current strengths of 8−13 nA/T. Very weak currents of 1.4−3.6 nA/T pass the NH unit of the conventional pyrrolic ring, when the second inner hydrogen is attached to a β-saturated one. Thus, for them, the inner NH unit functions as an inert bridge of the aromatic chlorin and bacteriochlorin (vide infra). Almost all current flows along the inner path at rings C and D, respectively, because of the saturated β carbons. The current density for the chlorins, depicted in Figure 7, shows that the diatropic ring current flows mainly along the outer edge of the molecules and the paratropic one on the inside of the macroring, as for porphin.

3.2.3. Bacteriochlorins. Bacteriochlorins have two pyrrolic rings saturated in the β positions. The current strength and current pathways have been calculated for four bacteriochlorin tautomers with the inner hydrogens and the β-saturated pyrrolic rings in *cis* or *trans* positions. The main ring-current branch avoids the saturated β carbons and the inner hydrogen, when that is possible. Thus, the bacteriochlorins have a very similar kind of ring-current pathways around the macroring as
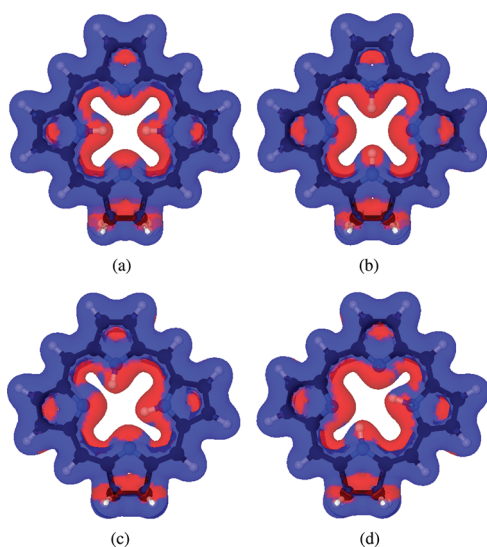
Figure 7. Magnetically induced current density calculated for *trans*-chlorin (a) t-CH$_2$-a, (b) t-CH$_2$-b and *cis*-chlorin (c) c-CH$_2$-a, (d) c-CH$_2$-b. Diatropic currents are shown in blue and paratropic currents in red.

Table 3. Strength of the Magnetically Induced Currents (in nA/T) Flowing around the Macroring as well as along the C=C (or C−C) and C−N−C routes of the Pyrrolic Rings of *trans*-Bacteriochlorin (t-BCH$_2$-a, t-BCH$_2$-b), *trans*-Isobacteriochlorin (t-IBCH$_2$), and *cis*-Bacteriochlorin (c-BCH$_2$)[a]

molecule	ring	macroring	route	
			C−N−C	C=C
t-BCH$_2$-a	A^H	23.1	4.8	18.3
	C	23.2	22.6	0.6
t-BCH$_2$-b	B	18.4	6.7	11.7
	D^H	18.6	19.5	−0.9
c-BCH$_2$	A^H	20.0	2.3	17.7
	B	20.0	7.8	12.2
	C	20.1	19.3	0.8
	D^H	20.1	20.6	−0.5
t-IBCH$_2$	A^H	14.7	0.3	14.4
	B	14.7	3.7	11.0
	C	14.9	13.8	1.1
	D^H	15.0	15.2	−0.2

[a]The A−D labeling of the pyrrolic rings is given in Figure 3. Pyrrolic rings with inner hydrogens are denoted by a superscript H.

the chlorins. However, an exception is seen for the pyrrolic rings labeled B without an inner hydrogen; the current is still branched, but it is not equally split. A preference of the outer route is observed. The main current pathways are depicted in Figure 3. The strongest ring current of 23.2 nA/T is obtained for t-BCH$_2$-a because the ring current does not have to pass any inner hydrogen at the β-saturated pyrrolic rings. The weakest ring current of 14.7 nA/T was obtained for t-IBCH$_2$, which has adjacent β-saturated rings and the inner hydrogen in *trans* position, implying that the ring current has to pass an NH unit. Even though the ring current passes one and two inner hydrogens in t-BCH$_2$-b and c-BCH$_2$, respectively, the net ring-current strengths of 18.6 and 20.1 nA/T are almost the same, but they are 3−5 nA/T smaller than for t-BCH$_2$-a, which has no inner hydrogens at the β-saturated rings. When one inner hydrogen is attached to a β-saturated pyrrolic ring, the second NH unit of a conventional pyrrolic ring is not part of the aromatic pathway as for the similar chlorins. The current strengths along the different pathways are given in Table 3. The current densities are depicted in Figure 8. The diatropic ring current flows mainly along the outer edge and the paratropic one inside the macroring as for the porphins and the chlorins.

3.2.4. Porphynoids with Three β-Saturated Pyrrolic Rings. The fourth set of porphynoids consists of molecules with three β-saturated pyrrolic rings and one conventional one. The calculated ring-current strengths for t-3BCH$_2$-a and t-3BCH$_2$-b are 13.0 and 15.5 nA/T, respectively, which shows that they are aromatic according to the ring-current criterion. For t-3BCH$_2$-a the obtained current pathway agrees well with the expected one, namely that the ring current flows along the inner pathway, when the β carbons are saturated and mainly via the outer route when the pyrrolic ring is aromatic and has an inner hydrogen. For t-3BCH$_2$-b, the integrated current strengths show that the current prefers the inner routes at rings C and D and the outer route at ring B. The calculated current strengths for the selected bonds of t-3BCH$_2$-a and t-3BCH$_2$-b are given in Table 4. The current densities are shown in Figure 9 and the main current pathways in Figure 4.
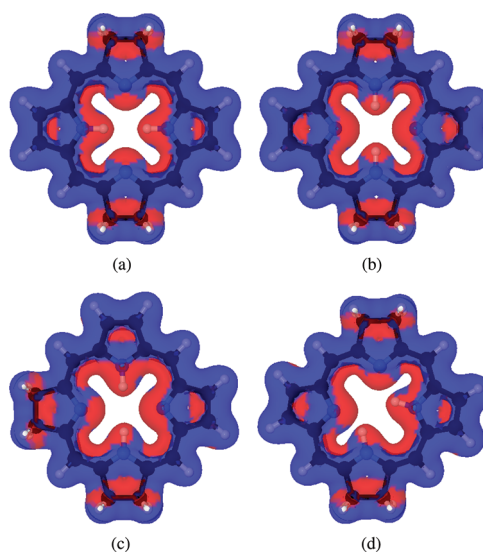

Figure 8. Magnetically induced current density calculated for *trans*-bacteriochlorin (a) t-BCH$_2$-a, (b) t-BCH$_2$-b, *trans*-isobacteriochlorin (c) t-IBCH$_2$, and *cis*-bacteriochlorin (d) c-BCH$_2$. Diatropic currents are shown in blue and paratropic currents in red.

3.2.5. Porphynoids with Four β-Saturated Pyrrolic Rings. For the porphynoid with all pyrrolic rings saturated in the β positions, the current flows along the inner cross pathway, which was suggested by Cyrañski et al. to be the aromatic pathway of porphin.[6] However, the current strength of 16.5 nA/T shows that t-4BCH$_2$ is aromatic but significantly less aromatic than porphin because the current has to pass the two inner NH sites, which have higher resistance than the N sites of the pyrrolic rings. The ring-current strength sustained in the inner cross is 67% of the ring-current strength for t-PH$_2$. The main current pathway and current density are depicted in Figure 4 and Figure 9, respectively, where one can see that the ring current flows along the outermost edge of the conjugated part of the porphynoid macroring.

Table 4. Strength of the Magnetically Induced Currents (in nA/T) Flowing around the Macroring as well as along the C═C (or C−C) and C−N−C Routes of the Pyrrolic Rings of t-3BCH$_2$-a, t-3BCH$_2$-b, and t-4BCH$_2$[a]

molecule	ring	macroring	route	
			C−N−C	C═C
t-3BCH$_2$-a	A[H]	12.7	−1.8	14.5
	C	12.9	12.1	0.8
	D[H]	13.0	13.2	−0.2
t-3BCH$_2$-b	B	15.2	2.2	12.9
	C	15.5	14.6	0.9
	D[H]	15.5	16.2	−0.7
t-4BCH$_2$	C	16.5	16.1	0.4
	D[H]	16.5	17.7	−1.2

[a]The A−D labeling of the pyrrolic rings is given in Figure 4. Pyrrolic rings with inner hydrogens are denoted by a superscript H.
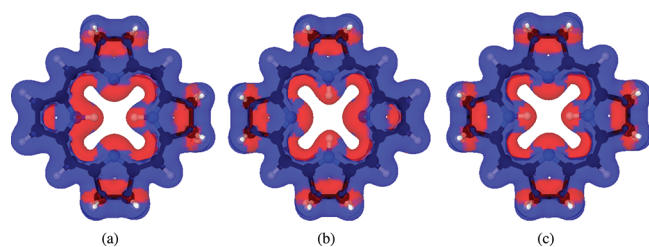

Figure 9. Magnetically induced current density calculated for the investigated 3-fold and 4-fold β-saturated *trans*-porphynoids (a) t-3BCH$_2$-a, (b) t-3BCH$_2$-b, and (c) t-4BCH$_2$. Diatropic currents are shown in blue and paratropic currents in red.

4. SUMMARY AND CONCLUSIONS

The magnetically induced current density has been calculated for free-base porphynoids using the gauge including magnetically induce current (GIMIC) method. Numerical integration of the current density passing selected chemical bonds yields the preferred current pathways. The strength of the ring current flowing around the planar porphynoid macrorings is used for assessing the degree of aromaticity according to the magnetic criterion. The present calculations on porphins, chlorins, and bacteriochlorins show that they are all aromatic according to the ring-current criterion. The ring-current strengths of the studied porphynoids are 1.5−2.5 times the one obtained for benzene. The integrated current strengths are significantly larger than those estimated from the calculated long-range magnetic shieldings using the ARCS method.[12] The pyrrolic rings sustain very weak ring currents, which cannot explain the increase in the long-range magnetic shieldings above the rings.

For most of the investigated porphynoids, the ring currents flow along all conjugated bonds of the porphynoids. The ring current branches at the pyrrolic rings taking both the outer and the inner route. The NH unit of the pyrrolic rings has a larger resistance and consequently a weaker current strength than the pyrroles without inner hydrogens. For β-saturated porphynoids, less than 5 nA/T of the ring current passes the NH unit when the ring current has the possibility to take the outer route at the pyrrolic ring. For t-IBCH$_2$ and t-3BCH$_2$, a weak current passes the N unit of the pyrrolic ring with unsaturated β carbons.

The porphins have the strongest ring current of ca. 27 nA/T among the investigated porphynoids. The ring current is split into two pathways at the pyrroles. At the pyrroles without an inner hydrogen, the current strengths of the two branches are practically equal, whereas the inner hydrogen of the pyrroles prevents to some extent the current to pass that way. The porphynoids with an inner hydrogen at the β saturated rings, which forces the ring current to take the inner route, have ring currents that are ca. 5 nA/T weaker than for the porphynoids, whose ring current can avoid the NH bridges. The ring-current strength of the bacteriochlorins are as strong as for the chlorins, whereas isobacteriochlorin sustains a somewhat weaker ring current of 14.7 nA/T. Isobacteriochlorin seems to belong to the same class as the 3-fold and 4-fold β-saturated porphynoids, as far as the net ring-current strength is concerned.

The GIMIC calculations yield unambiguous current pathways and novel insights of the aromaticity of porphyrins. The calculations show that the 18π [16]annulene inner cross is not the correct picture of the aromatic pathway for porphyrins. The traditional 18π [18]annulene with inactive NH units is not how the ring-current flows around the macroring either. All conjugated chemical bonds of porphyrins participate in the current transport around the macroring.

■ ASSOCIATED CONTENT

Ⓢ Supporting Information

Cartesian coordinates and nuclear magnetic shieldings of the studied molecules. This material is available free of charge via the Internet at http://pubs.acs.org.

■ AUTHOR INFORMATION

Corresponding Author
*E-mail: heike@fliegl.org; dage.sundholm@helsinki.fi.
Notes
The authors declare no competing financial interest.

■ ACKNOWLEDGMENTS

■ REFERENCES

(1) Vogel, E.; Haas, W.; Knipp, B.; Lex, J.; Schmickler, H. *Angew. Chem., Int. Ed.* **1988**, 27, 406−409.
(2) Vogel, E. *J. Heterocycl. Chem.* **1996**, 33, 1461−1487.
(3) Lash, T. D.; Chaney, S. T. *Chem.—Eur. J.* **1996**, 2, 944−948.
(4) Lash, T. D.; Romanic, J. L.; Hayes, J.; Spence, J. D. *Chem. Commun.* **1999**, 819−820.
(5) Steiner, E.; Fowler, P. W. *Chem. Phys. Chem.* **2002**, 3, 114−116.
(6) Cyrański, M. K.; Krygowski, T. M.; Wisiorowski, M.; van Eikema Hommes, N. J. R.; von Ragué Schleyer, P. *Angew. Chem., Int. Ed.* **1998**, 37, 177−180.
(7) von Ragué Schleyer, P.; Maerker, C.; Dransfeld, A.; Jiao, H.; van Eikema Hommes, N. J. R. *J. Am. Chem. Soc.* **1996**, 118, 6317−6318.
(8) Krygowski, T. M. *Chem. Inf. Comput. Sci.* **1993**, 33, 70−78.
(9) Havenith, R. W. A.; Meijer, A. J. H. M.; Irving, B. J.; Fowler, P. W. *Mol. Phys.* **2009**, 107, 2591−2600.
(10) Lloyd, D. *J. Chem. Inf. Comput. Sci.* **1996**, 36, 442−447.
(11) von Ragué Schleyer, P.; Jiao, H. *Pure Appl. Chem.* **1996**, 28, 209−218.
(12) Jusélius, J.; Sundholm, D. *Phys. Chem. Chem. Phys.* **2000**, 2, 2145−2151.
(13) Jusélius, J.; Sundholm, D. *Phys. Chem. Chem. Phys.* **1999**, 1, 3429−3435.
(14) Jusélius, J.; Sundholm, D. *J. Org. Chem.* **2000**, 65, 5233−5237.
(15) Setsune, J.; Maeda, S. *J. Am. Chem. Soc.* **2000**, 122, 12405−12406.

(16) Shin, J. Y.; Furuta, H.; Igarashi, S.; Osuka, A. *J. Am. Chem. Soc.* **2001**, *123*, 7190−7191.

(17) Sprutta, N.; Latos-Grażyński, L. *Chem.—Eur. J.* **2001**, *7*, 5099−5112.

(18) Setsune, J.; Katakami, Y.; Iizuna, N. *J. Am. Chem. Soc.* **1999**, *121*, 8957−8958.

(19) Stepień, M.; Szyszko, B.; Latos-Grażyński, L. *Org. Lett.* **2009**, *11*, 3930−3933.

(20) Stepień, M.; Latos-Gra]yński, L.; Sprutta, N.; Chwalisz, P.; Szterenberg, L. *Angew. Chem., Int. Ed.* **2007**, *46*, 7869−7873.

(21) Stepień, M.; Szyszko, B.; Latos-Grażyński, L. *J. Am. Chem. Soc.* **2010**, *132*, 3140−3152.

(22) Stepień, M.; Sprutta, N.; Latos-Grażyński, L. *Angew. Chem., Int. Ed.* **2011**, *50*, 4288−4340.

(23) Yoon, Z. S.; Osuka, A.; Kim, D. *Nature Chem.* **2009**, *1*, 113−122.

(24) Tanaka, Y.; Saito, S.; Mori, S.; Aratani, N.; Shinokubo, H.; Shibata, N.; Higuchi, Y.; Yoon, Z. S.; Kim, K. S.; Noh, S. B.; Park, J. K.; Kim, D.; Osuka, A. *Angew. Chem., Int. Ed.* **2008**, *47*, 681−684.

(25) Rappaport, S. M.; Rzepa, H. S. *J. Am. Chem. Soc.* **2008**, *130*, 7613−7619.

(26) Sankar, J.; et al. *J. Am. Chem. Soc.* **2008**, *130*, 13568−13579.

(27) Rzepa, H. S. *Org. Lett.* **2008**, *10*, 949−952.

(28) Jux, N. *Angew. Chem., Int. Ed.* **2008**, *47*, 2543−2546.

(29) Saito, S.; Shin, J. Y.; Lim, J. M.; Kim, K. S.; Kim, D.; Osuka, A. *Angew. Chem., Int. Ed.* **2008**, *47*, 9657−9660.

(30) Wannere, C. S.; Rzepa, H. S.; Rinderspacher, B. C.; Paul, A.; Allan, C. S. M.; Schaefer, H. F. III; von Ragué Schleyer, P. *J. Phys. Chem. A* **2009**, *113*, 11619−11629.

(31) Stepień, M.; Latos-Grażyński, L. Aromaticity and Tautomerism in Porphyrins and Porphyrinoids. In *Aromaticity in Heterocyclic Compounds*; Krygowski, T., Cyranski, M., Eds.; Springer: Berlin/Heidelberg, 2009; Vol. 19, pp 83−153.

(32) Bröring, M. *Angew. Chem., Int. Ed.* **2011**, *50*, 2436−2438.

(33) Aihara, J.; Makino, M. *Org. Biomol. Chem.* **2010**, *8*, 261−266.

(34) Higashino, T.; Lim, J. M.; Miura, T.; Saito, S.; Shin, J.-Y.; Kim, D.; Osuka, A. *Angew. Chem., Int. Ed.* **2010**, *49*, 1−6.

(35) Fliegl, H.; Sundholm, D.; Taubert, S.; Pichierri, F. *J. Phys. Chem. A* **2010**, *114*, 7153−7161.

(36) Fliegl, H.; Sundholm, D.; Pichierri, F. *Phys. Chem. Chem. Phys.* **2011**, *13*, 20659−20665.

(37) Taubert, S.; Sundholm, D.; Pichierri, F. *J. Org. Chem.* **2009**, *74*, 6495−6502.

(38) Jusélius, J.; Sundholm, D.; Gauss, J. *J. Chem. Phys.* **2004**, *121*, 3952−3963.

(39) Taubert, S.; Sundholm, D.; Jusélius, J. *J. Chem. Phys.* **2011**, *134*, 054123:1−12.

(40) Fliegl, H.; Taubert, S.; Lehtonen, O.; Sundholm, D. *Phys. Chem. Chem. Phys.* **2011**, *13*, 20500−20518.

(41) Keith, T. A.; Bader, R. F. W. *Chem. Phys. Lett.* **1993**, *210*, 223−231.

(42) Coriani, S.; Lazzeretti, P.; Malagoli, M.; Zanasi, R. *Theor. Chim. Acta* **1994**, *89*, 181−192.

(43) Steiner, E.; Soncini, A.; Fowler, P. W. *Org. Biomol. Chem.* **2005**, *3*, 4053−4059.

(44) Steiner, E.; Fowler, P. W. *Org. Biomol. Chem.* **2006**, *4*, 2473−2476.

(45) Vosko, S. H.; Wilk, L.; Nusair, M. *Can. J. Phys* **1980**, *58*, 1200−1211.

(46) Perdew, J. P. *Phys. Rev. B* **1986**, *33*, 8822−8824.

(47) Becke, A. D. *Phys. Rev. A* **1988**, *38*, 3098−3100.

(48) Eichkorn, K.; Treutler, O.; Öhm, H.; Häser, M.; Ahlrichs, R. *Chem. Phys. Lett.* **1995**, *240*, 283−289.

(49) Schäfer, A.; Horn, H.; Ahlrichs, R. *J. Chem. Phys.* **1992**, *97*, 2571−2577.

(50) Dunning, T. H. Jr. *J. Chem. Phys.* **1989**, *90*, 1007−1023.

(51) Becke, A. D. *J. Chem. Phys.* **1993**, *98*, 5648−5652.

(52) Lee, C.; Yang, W.; Parr, R. G. *Phys. Rev. B* **1988**, *37*, 785−789.

(53) Weigend, F.; Ahlrichs, R. *Phys. Chem. Chem. Phys.* **2005**, *7*, 3297−3305.

(54) Ahlrichs, R.; Bär, M.; Häser, M.; Horn, H.; Kölmel, C. *Chem. Phys. Lett.* **1989**, *162*, 165−169.

(55) London, F. *J. Phys. Radium* **1937**, *8*, 397−409.

(56) Hameka, H. F. *Mol. Phys.* **1958**, *1*, 203−215.

(57) Ditchfield, R. *Mol. Phys.* **1974**, *27*, 789−807.

(58) Wolinski, K.; Hinton, J. F.; Pulay, P. *J. Am. Chem. Soc.* **1990**, *112*, 8251−8260.

(59) Johansson, M. P.; Jusélius, J.; Sundholm, D. *Angew. Chem., Int. Ed.* **2005**, *44*, 1843−1846.

(60) Jusélius, J.; Sundholm, D. *Phys. Chem. Chem. Phys.* **2008**, *10*, 6630−6634.

(61) Lin, Y. C.; Jusélius, J.; Sundholm, D.; Gauss, J. *J. Chem. Phys.* **2005**, *122*, 214308:1−9.

(62) Fliegl, H.; Sundholm, D.; Taubert, S.; Jusélius, J.; Klopper, W. *J. Phys. Chem. A* **2009**, *113*, 8668−8676.

(63) Zanasi, R.; Lazzeretti, P.; Malagoli, M.; Piccinini, F. *J. Chem. Phys.* **1995**, *102*, 7150−7157.

(64) Lazzeretti, P. *Prog. Nucl. Magn. Reson. Spectrosc.* **2000**, *36*, 1−88.

(65) Gomes, J. A. N. F.; Mallion, R. B. *Chem. Rev.* **2001**, *101*, 1349−1384.

(66) JMOL: an open-source Java viewer for chemical structures in 3D, http://www.jmol.org.

(67) http://www.gnuplot.info/.

(68) http://www.gimp.org/.